Natural Hazards **27:** 61–84, 2002.

The Fault that Caused the Athens September 1999 Ms = 5.9 Earthquake: Field Observations

S. B. PAVLIDES[1], G. PAPADOPOULOS[2] and A. GANAS[2]
[1]*Department of Geology, University of Thessaloniki, 54006, Greece E-mail: Pavlides@geo.auth.gr;*
[2]*Geodynamics Institute, National Observatory of Athens, PO Box 20048, 11810 Athens, Greece*

Received: 18 October 2000; accepted in revised form: 5 November 2001

Abstract. On 7 September 1999 the Athens Metropolitan area (Greece) was hit by a moderate size (Ms = 5.9) earthquake. The severely damaged area is localized in the northwestern suburbs of the city, at the foothills of Mt. Parnitha (38.1°N, 23.6°E), about 18 km from the historic centre of Athens. In this paper, we present our results on the surface expression of the seismogenic structure. Methods applied were: field observations, geological mapping, fault geometry and kinematics, evaluation of macroseismic data, interpretation of LANDSAT images, construction of a DEM and application of shading techniques. Aftershock distribution and fault plane solutions were also considered. Our results suggest that the earthquake source is located within the NW-SE trending valley bearing a few outcrops of Neogene- Quaternary sediments across the south foothills of Mt. Parnitha, never known in the past to have been activated by such strong earthquakes. The earthquake occurred along a 10 km long normal fault, striking N110°–133° and dipping 64°–85°SW, extending from the Fili Fort (4th century BC) in the NNW to the Fili town and then to Ano Liossia, to the SSE. Tensional stress field with σ_3 axis almost horizontal striking NNE-NE prevails in the area. The fault strike and the extensional direction (σ_3) are compatible with the focal mechanism of the main shock.

1. Introduction

On 7 September 1999 at 14:56:50 local time (11:56:50 GMT) a moderate-size (Ms = 5.9) earthquake occurred in Attica (Greece) that inflicted heavy damage upon the Athens Metropolitan area, hitting a densely populated area. 143 lives were lost and 800 were injured. This is the highest number in Greece of the 20th century after the Ionian Sea 1953 earthquake, where 455 people were killed.

The focal parameters of the main shock are: Ms = 5.9 ($M_L = 5.4$), $\varphi N = 38.08°$, $\lambda E = 23.58°$, $h = 16.7$ km (Papadopoulos *et al.*, 2000, 2001). The epicentre and especially the depth of this event has been calculated slightly different by other institutes e.g., 11–14 km Geophys. Lab University of Thessaloniki, 8 km by the University of Athens (Papadimitriou *et al.*, 2000; Sargeant *et al.*, 2000), 11 km by Louvari and Kiratzi (2000), and 9 km by USGS. The area most severely hit was the municipality of Ano Liossia and Acharnai (Figures 1 and 2). The maximum intensity has been evaluated at Io - VIII and locally IX + (MSK). The recorded peak ground acceleration values vary from 0.02 to 0.32 g and in one case 0.50 g (?), at distance 15 to 20 km from the seismic source. These values

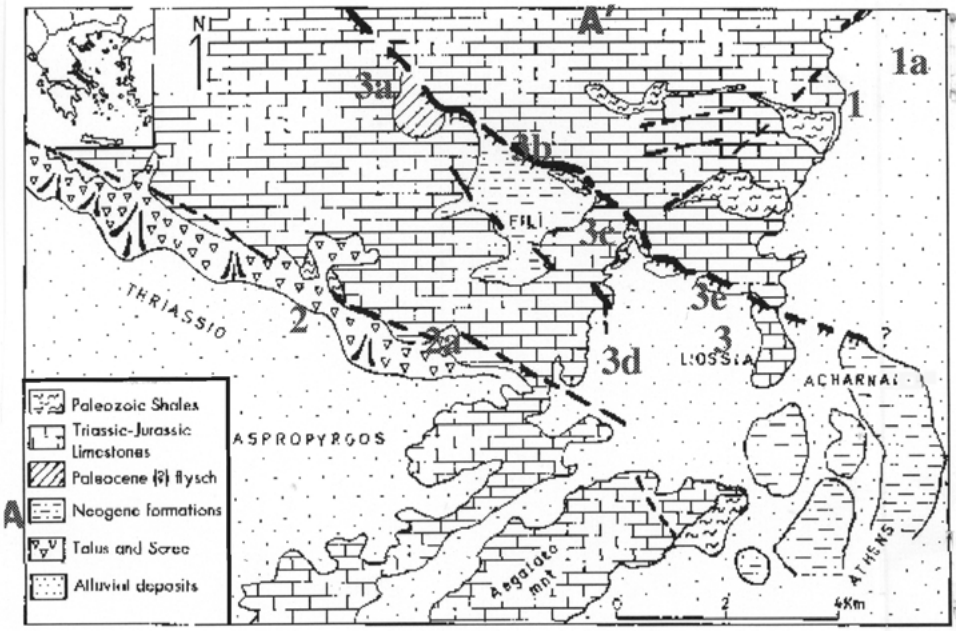

Figure 1. Simplified geological map of the study area (southern Parnitha mountain – western Attica district), where three normal neotectonic faults (1, 2, 3) are shown.

1. *NE-SW trending fault of the eastern marginal foothills of Mt. Parnitha (western Athens basin) as dashed line.*
2. Thriassion neotectonic fault *as dashed line*.
3. Fili fault, which is the possible seismogenic structure, as *thick line with ticks*.

(1a, 3a, 3b, 3c, 3e, 3d are sites of measurements-see Field Observations chapter – and AA′ the geological section of Figure 13).

are significantly higher than expected according to NEAK (New Greek Building Seismic Code – 1995). More than 1500 aftershocks were recorded by the NOA GI (National Observatory of Athens – Institute of Geodynamics) portable array deployed in the earthquake area (see also Papadopoulos *et al.*, 2000).

The earthquake was unexpected on account of two reasons: first, no major (longer than 10 km) active structure inside or close to the Athens basin was known and second, the seismicity of the Athens area has been very low during the last three millennia. Additionally, the epicentral area of southwestern Parnitha was not known as seismogenic. This is the greatest instrumentally recorded event in the Metropolitan area of Athens, a region which was considered to be “aseismic” or of “very low seismicity”, although the historical seismicity of the city has not been thoroughly known. The only known earthquake of similar size in the broader area of Athens is the 1705 event (Ambraseys, 1994). The failure to appreciate the hazard for Athens is not unique. Another large event (Ms 6.6) occurred in the Kozani-Grevena area in May 13, 1995 (Pavlides and King, 1998) within an “aseismic” area. In both cases the fault system responsible for the event had not been identified

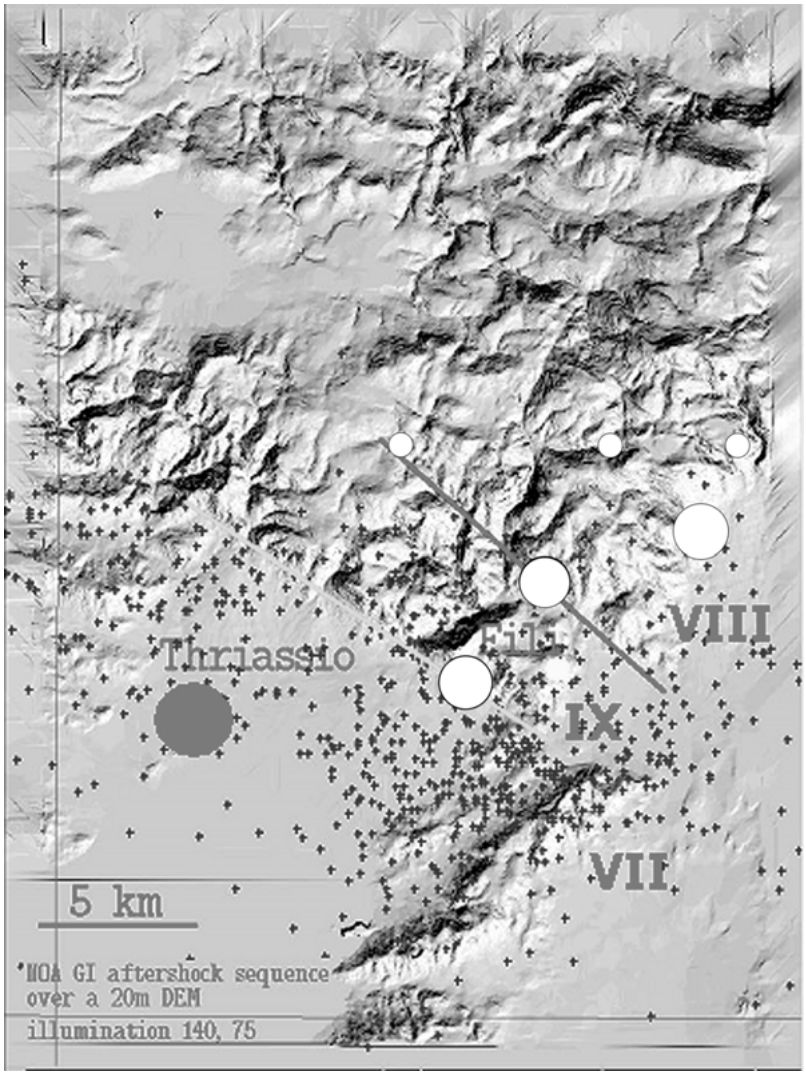

Figure 2. Shaded relief image of a Digital Elevation Model (DEM) of the epicentral area simulating orientation of topography with respect to an illumination source (SE-140; zenith angle of 75 degrees), where the spatial distribution of the aftershocks is shown too. Light line is the Thriassion normal fault heavy dark line is the Fili normal fault. Crosses are aftershock epicenters provided by Papadopoulos *et al.* (2000, 2001). Stars are the preliminary and relocated NOAGI epicenters of the main shock of September 7, 1999. Map shows also schematically the distribution of rockfalls mainly and other macroseismic phenomena (dots). Roman capital letters indicate the earthquake intensity.

previously. In this respect, the earthquake can be characterized as a "floating" or "random event" (de Polo and Slemmons, 1990). "Floating" earthquakes are usually small-to-moderate events (magnitude range 5 to 6.5) that can occur anywhere in a region or area. This is the case of the Athens shock.

The identification of the seismogenic fault is of great significance to understand better the seismic process and to evaluate more reliably the seismic hazard of the area. There was a great uncertainty and confusion among the geoscientists about which was the fault that caused the earthquake and there is still no agreement. In general, the fault that caused the shock was believed to be a deep structure that does not reach the surface, without topographic expression. For this reason the term "blind fault" has been introduced. But, when studied, the geological structures in the region are identifiable as active or possibly active on the basis of the pre-earthquake morphology. In general, it is now clear that earthquakes produce permanent and recognizable effects on the landscape, which can enable geologists to infer the degree of seismic activity in a region (see Pavlides and King, 1998), especially in continental Greece, where small and scattered normal faults produce medium and strong (Ms = 6 to 7) events. Faults that are small, often show features that are scale invariant over some part of their size range (Jackson, 1999). Few earthquakes with Ms as small as 5.7 have been observed in Greece, clearly associated with seismogenic faults and giving rise to surface faulting (Ambraseys and Jackson, 1990; Stiros, 1995). Recent studies on the September–October 1997 earthquake sequence (Ms 5.5 to 5.9) in Umbria-Marche (central Italy) have shown co-seismic rupture a few meters long along a total length of 5 km with a displacement of 2–20 cm (Galli and Galadini, 1999; Meghraoui *et al.*, 1999; Vittori *et al.*, 2000). Michetti *et al.* (2000) refers to ground effects caused by the Mw = 5.6 on 9 September, 1998 Lauria earthquake (Southern Italy), too. Coppersmith and Young (2000), based on worldwide data, suggest that an earthquake with magnitude 6.0 has about 25% of probability to produce surface co-seismic ruptures. But small-moderate events have not been observed or studied systematically worldwide.

The tools which have been used to identify the seismic source in this study are: field observations mainly (neotectonic and morphotectonic) undertaken in the first few weeks after the earthquake, the existing geological map information (Athena–Elefsis sheet 1:50.000, IGME 1980), LANDSAT satellite imagery acquired in 1993, Digital Elevation Models (3D topography) constructed from a general use map of 1992, macroseismic data (intensities), rock falls and other ground deformation, focal mechanisms and aftershock distribution as derived from the portable seismographs by NOAGI.

2. Geology and Neotectonics of the Region

The basement rocks of the epicentral area, on the southern side of Mt Parnitha, are Paleozoic shales and sandstones in alternation with phylites and quartz conglom-

erates, Triassic-Jurassic crystalline carbonate rocks, dolomites and few outcrops of Cretaceous limestone and Paleocene (?) flysch (turbidites) of the Pelagonian geotectonic zone. Neogene formations at the Fili small depression (syn-rift deposits) overlie unconformably the basement formations and consist of alternating beds of marls, lacustrine limestone, marls and sandstones. Quaternary deposits are unconsolidated sandy-clayey soils, talus cones and scree materials. According to Freyberg (1951), the oldest post-alpide deposits in the western part of the Athens Basin, are also lacustrine marls and clays with lignite strata of late Miocene age. Pliocene formation are clays too, sands and sandstones, gravels in alternation with white limestone, which very likely pass over to Pleistocene. These deposits have a considerable thickness more than 300 to 400 m (Freyberg, 1951), especially in the area of Acharnai where exceptionally high values of seismic intensities (IX) were locally observed.

The pre-existing inherited structures, that are zones of weakness, are Cretaceous thrusts of Paleozoic formations onto Triassic–Jurassic carbonate formation, from top to the west, as well as younger, post-alpide normal faults. These faults are minor structures striking both NE-SW and WNW-ESE. The neotectonic pattern consists of highs and depressions of similar trends. The Athens basin, which is the main and great neotectonic feature in Attica, is elongated NE-SW, while other neotectonic depressions like the Thriassion–Aspropyrgos and the small Fili basin are elongated NW-SE. It is worth to note that, according to Freyberg's (1951) map, the Fili fault extends towards the Athens Basin under the Ano Liossia and Acharnai suburbs.

The normal faults of Thriassion and Fili dominate the area, and especially the first one, are clearly visible in aerial photographs and LANDSAT images. These are WNW-ESE trending, SE dipping structures (Figures 1, 2). The first fault is also the northern border of Thriassion (or Aspropyrgos) basin and is covered by typical talus cones and scree. An almost parallel segment lies 5 km to the northeast. This is the Fili fault shown in the IGME geological map as bordering to the north of the small Neogene basin of Fili, as a 5 km long structure in close relation with alpide thrusts. The Thriassion fault terminates against the transverse crystalline limestone ridges of the Aegaleo Mountain, while the Fili fault very possibly extends towards the Athens Basin. Based on their morphotectonic features, both normal NW-SE trending faults could be considered as "possible active structures". Additionally, it is known that the change in activity from faults with NW-SE to E-W strikes in Central Greece happened within the last $\sim$1 Ma (Leeder and Jackson, 1993; Jackson, 1999).

The third marginal fault of the Athens basin, striking NE-SW, is covered by characteristic alluvial fans (Figure 1). Only a few outcrops and mainly eroded fault surfaces exist along it. It shows no signs of late Quaternary or Holocene activity.

The Fili fault is normal to the structural trend of the Athens basin (NE-SW) and cuts Mesozoic limestone and Paleozoic metamorphic rocks. The Neogene formations found at its hanging wall are also affected by minor faults of similar geometry.

In several cases, where we mapped normal dip-slip fault movements, they follow old thrust planes or they were parallel and close to them, implying that they used the pre-existing thrusts as zones of weakness. However, this is not always the case and more mapping needs to be undertaken to examine the structural relationship between active faulting and Cretaceous thrusting.

3. Instrumental Records and Focal Mechanisms – a Review

Reliable preliminary fault plane solutions for the main shock were determined automatically by USGS, CALTECH, HARVARD and others. They clearly show WNW-ESE trending nodal planes (NP), which have dip-slip normal components, and extensional regime: axis P vertical, axis T horizontal NE-SW trending.

USGS NP1: strike = 123, Dip = 55, Slip = −84 NP2: 292, 36, −99

CALT NP1: strike = 122, Dip = 60, Slip = −80, NP2: 282, 31, −107

HARV NP1: strike = 114, Dip = 45, Slip = −73, NP2: 271, 47, −106

We also utilized the focal mechanism determined by Louvari and Kiratzi (2001) based on body wave modeling of teleseismic waves from first motion polarities of P-waves, which were recorded at GDSN stations with epicentral distances $30^\circ < \Delta < 90^\circ$. They used far-field body waveform modeling and displacement spectral analysis to study the source parameters of the 7 September 1999 Athens earthquake (Mw = 5.9). Both P and SH teleseismic waveforms were used in the analysis, and the inset in Figure 3 shows the results of their modelling. Accordingly, the earthquake was caused by the motion of a high-angle normal fault with: Strike = 115° dip = 57°, rake = −80°, auxiliary plane with strike = 277°, dip = 34°, rake = − 105°.

The source time function reveals source duration of 4.2 s, while more than 95% of the energy was abruptly released within the first 2.2 s. The scalar seismic moment was found equal to 9.22×10^{17} Nm. The spectral analysis, assuming a rectangular fault, yielded fault length, L = 18 km, fault width, w = 10 km, stress drop, $\Delta\sigma$ = 9 bar, and average dislocation, $\bar{u}$ = 30 cm, and focus depth at 11 km. These values are in agreement with those expected from the empirical scaling relations applicable to Greece (Louvari and Kiratzi, 2000).

Similar results for the seismogenic fault come from the focal mechanism determined by Athens University and NOAGI :

Azimuth 105°; Dip 55° SW, Rake −80°; normal (Papadimitriou *et al.*, 2000)

Azimuth 113°; Dip 39° SW, Rake −90°; normal (Papadopoulos *et al.*, 2000)

We consider this solution to represent movement either along the Fili or Thriassion faults because the first nodal plane is parallel to them and dips SW in

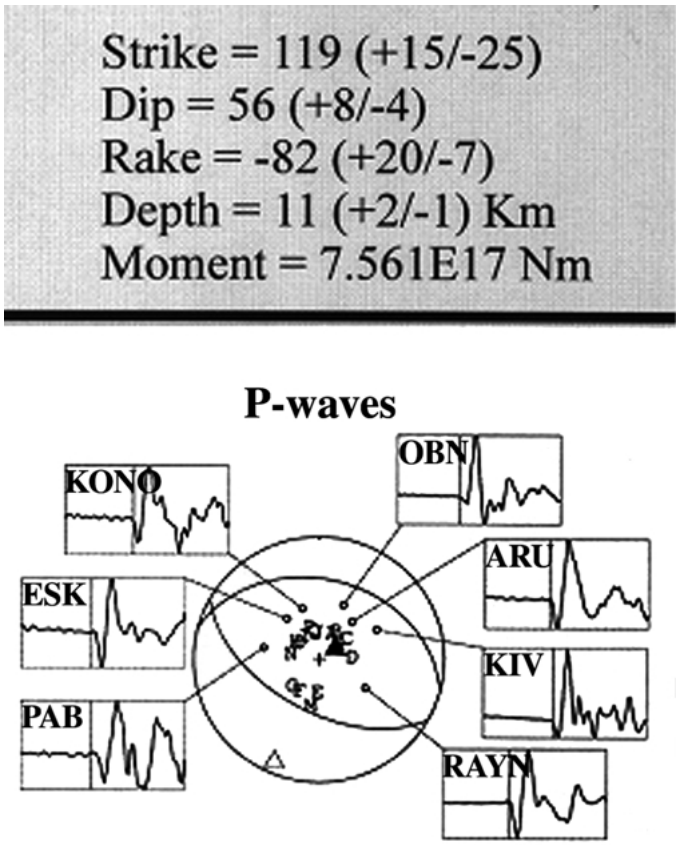

Figure 3. Fault plane solution (after Louvari and Kiratzi, 2001). The WNW-ESE trending and SW dipping faults fit the field measurements for Fili and Thriassion faults.

consistency with the tectonic regime of the area (Figure 3). Besides, the above fault planes are also characterized by high dip angles as expected for normal faults. In addition, the spatial distribution of aftershock foci indicates that the Fili normal fault defines better the seismic source. Figure 2 shows 800 aftershocks determined by NOAGI by the end of October 1999 plotted on the geocoded elevation model. In the same figure other data (such as macroseismic information regarding rock falls and gravitational cracks) are also plotted (Figure 2). A 3D extrapolation of the spatial distribution of the aftershocks' hypocenters, as derived from Papadopoulos *et al*. (2000), as well as from Voulgaris *et al.* (2000) and Tselentis and Zahradnik (2000), indicates that the actual surface fault line is located within the Fili fault. Additionally, Sargeant *et al.* (2000) describe a normal fault mechanism with a small component of left lateral strike-slip, which is consistent with our field measurements. The rupture radius (6.5 km) and the focal depth (8 km) do not combine to produce surface rupture. The stress drop is low (1.1 MPa), so the

formal continuation of the fault plane to the free surface intersects near Fili fault, suggesting that this was the causal fault (Sargeant *et al.*, 2000).

4. DEMs and Landsat Image Interpretation

A Landsat 5 Thematic Mapper sub-scene (acquisition 14 September 1993 – path 183 row 33) was used to identify the neotectonic features of the area. The spatial resolution of this sensor is 30 m. The scene was provided by Eurimage SA (Rome, Italy) with a minimum level of radiometric and geometric pre-processing, including its transformation to the UTM projection system. Radiometric corrections are applied by use of calibration coefficients to each individual detector in the satellite sensor. Then, the image was georeferenced to the Greek national projection system EGSA 1987 by use of the EASI PACE v6.3 software. The ground control points were collected from recent 1:50,000 topographic maps. The RMS error of the correction measured on the ground control points was less than a pixel (30 m). A digital elevation model (DEM) was also produced by on-screen digitising of elevation contours of the 1:50,000-map sheet "Elefsis" (contour interval 20 m). The model was georeferenced to the Greek national grid by a 2nd order polynomial transformation and was constructed at 20 m pixels to eliminate interpolation errors in image space between the contours (the procedure is described in Ganas and Athanassiou, 2000). Then, shaded relief images in greyscale were produced using various illumination conditions in order to study the long-term evolution of landforms in the meisoseismal area. The shaded relief image (Figure 2) that simulates a low sun angle, southeastern viewing direction, can be used as a raster background to overlay vector files like the aftershock sequence provided by NOAGI. Additionally, this map shows better the relief of the epicentral area, where the dominant features seen on the shaded relief image close to the aftershock sequence again are the two NW-SE normal faults of Thriassion and Fili downthrown to the SW. Other parallel to sub-parallel features of tectonic origin occur only to the north (10–15 km) of the epicentral area. In addition, no NE-SW faults are seen to crosscut the Fili fault.

The most impressive structure in the 3D image is the Thriassion normal fault (Figure 4), due to its linearity and its relief. However, this fault in the field does not show typical morphotectonic features and looks "old", as it is characterised by eroded scarps, undisturbed alluvial fans and scree sediments. The smaller Fili fault is expressed as an abrupt linear front for a distance of about 6 km in the general NW- SE direction (Figure 4). The good alignment of ridges against this front indicates that the fault is active and dips to the SW. In the area to the north of Fili town, the fault can be traced cutting the oblique, "Alogorachi" limestone ridge and continuing to the NW, with the ancient fort of Fili located in its hangingwall. From remote sensing its visible length is estimated to be about 8-10 km.

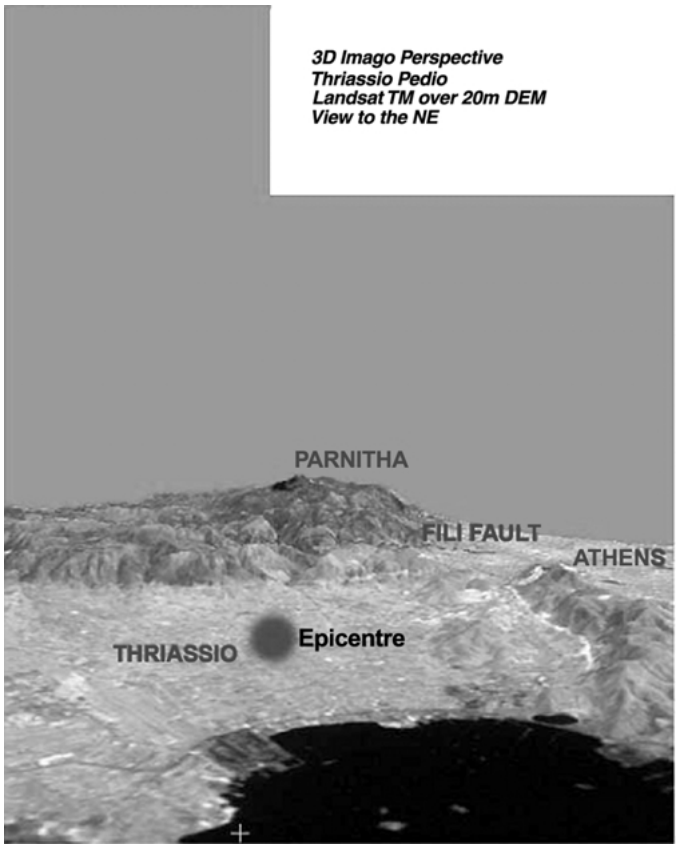

Figure 4. Three dimensional view of the 7 September 1999 epicentral area of Athens Earthquake. The image was constructed using computer vision techniques, satellite imagery and a digital elevation model (DEM). Heavy line is the trace of the Fili normal fault that moved during the 7 September 1999 earthquake.

5. Field Observations

Due to the moderate size of the event, no typical, continuous, co-seismic ruptures were found. This makes it difficult to determine which was the active fault that caused the M 5.9 earthquake without taking into account other evidence. A piece of evidence may be provided by the length of the segment, as predicted by empirical relationships. Fault lengths can be predicted by Wells and Coppersmith (1994), Ambraseys and Jackson (1998) and Pavlides *et al.* (2000a) formulae comparing Magnitude (M) versus Surface Rupture Length (SRL) and Maximum – Average Displacement (MD and AD). According to M-SRL and M-MD relationships, the surface fault length is expected in the ranges of 5 to 8 km and the co-seismic displacement 0 to 6 cm, respectively. Hence, a Mw = 5.9–6.0 (Ms = 5.6–5.8) event is marginal in producing surface ruptures. As a consequence, additional geological observations have been collected, concerning all the neotectonic structures of the

area, that is, central, eastern and southern Parnitha Mountain, where the density of ground failures, like rock falls and gravitational cracks, were high.

5.1. MACROSEISMIC EVIDENCE – ROCK FALLS

Seismic damages include extensive building collapses that are concentrated on the eastern extension of the seismogenic fault (Ano Liossia, Acharnai and other suburbs of the western Athens – Figure 2), and along the Fili fault (Fili town and Fili castle of 4th century BC). Soil amplification effects were also responsible for extensive damage along this direction because of the occurrence of (a) soft lacustrine beds and (b) recent alluvial deposits. On the other hand, there are "site effects" which need further investigation, especially from an engineering point of view. The Fili castle, established in the 4th century BC, is located at the NW part of the epicentral area. It suffered a lot of damage, such as wall collapses, cracks and falls of structural elements, evidence of its proximity to the earthquake epicenter. The town of Fili was also struck, with half of its buildings marked "for repair works" and many "for demolition". Ano Liossia and Acharnai, on the ESE extension of Fili fault, are the urban areas with highest observed intensities (VIII to IX locally). An exceptional area with serious damages is the Thrakomakedones suburb, lying on the NE-Athens basin marginal fault.

In the area bounded by the Thriassion fault (Thriassion Pedion – Aspropyrgos basin) the damage was less extensive. The fault did not show co-seismic deformation. Unconsolidated sediments, talus cones and colluvium remained intact and unbroken with the exception of rock falls shown in Figures 2 and 5. Neither an active landslide rejuvenated, nor the water supply pipeline showed any movements due to primary fault effects or to shaking. No typical Holocene scarps exist within the fault. Furthermore, the towns of Salamis and Aspropyrgos lying 5–8 km to the south of the Thriassion fault (in its hangingwall), suffered much less than other suburbs of Athens, the intensity not exceeding V to VI degrees.

Rock falls were widespread on the whole central and especially southeastern Parnitha area (see Figures 2 and 5). In most cases rock falls are directly associated to pre-existing discontinuities and steep slopes within the crystalline limestone.

5.2. DESCRIPTION OF SURFACE RUPTURES

We searched for surface ruptures on the entire epicentral area. Various freshly exposed earthquake induced dislocations were observed and were examined in detail (see locations 1a, 3a, 3b, 3c, 3d on the map of Figure 1).

- Minor ground gravitational cracking, was mapped in the ancient Fili Fort (4th century B.C – location N38°08′29″, E023°38′13″) (Figure 1, site 3a). The castle wall, consisting of carbonates rectangular big stones, partly collapsed and the foundations cracked. The average strike of fissures was NNE-SSW to N-S. Very close to the castle, at the WNW extension of the Fili fault,

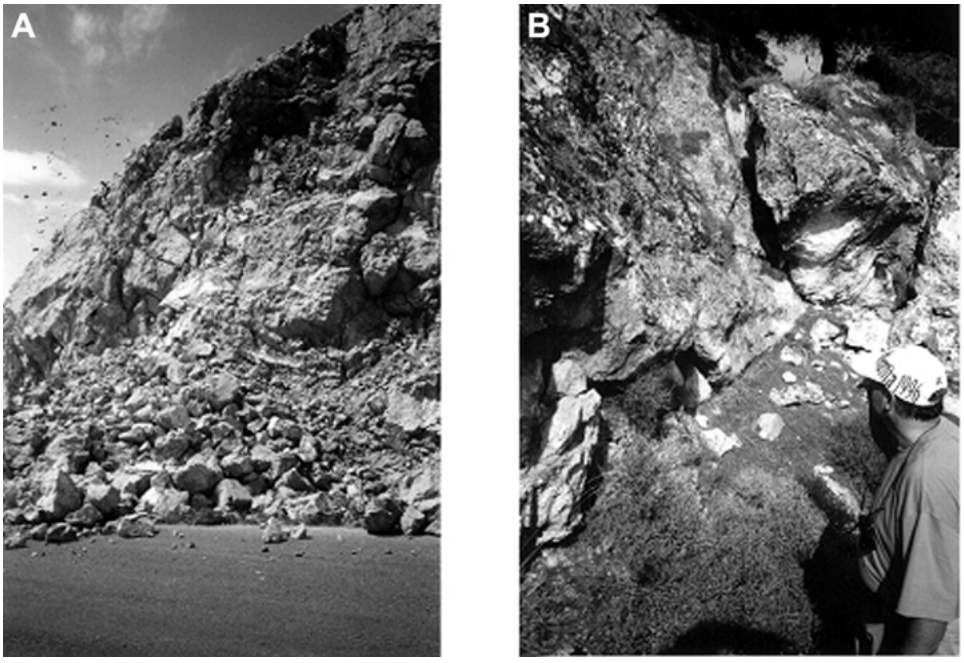

Figure 5. (a) rock falls close to the Triassion fault (see Figure 1, site 2a for location). (b) field photograph of a gravitational limestone block separation and displacement along a small neotectonic fault surface, antithetic to the Fili fault at Ano Liossia to Fili town (for location, see Figure 1, site 3d).

(strike 100–120°) bedrock small fault scarps were observed. Light bands (D about 10 cm) on the carbonate fault surfaces were detected (Figure 6). The "freshness" of the bedrock cropping out along the strip, the lack of weathering on it, in contrast to the bedrock surface above, indicate "older", but still very young, possibly historical co-seismic reactivation of the fault (see also Jackson *et al.*, 1982; Stewart and Hancock, 1988, 1991; Stewart, 1993; Caputo, 1993 and others)

- A well developed WSW-ESE (N100°–N130°) trending and 64° to 90° SW dipping fault scarp within the crystalline carbonate rocks is exposed northwestern of Fili town along the homonym fault. This is a well expressed polished fault surface, that is a fresh non weathered surface, up to 10 m high, typical of active faults, known also from other seismogenic faults (e.g., Jackson *et al.*, 1982). That is the well-known Aegean type, typical characteristic, morphology of active faults (see Stewart and Hancock, 1988, 1991). The observed dislocations extend along a total length of about 100 m, are open fissures (1–2 cm) and show variable vertical displacements (6–10 cm). The ruptures affected mainly basement rock and some very thin loose deposits. (Figure 1, site 3b and Figures 6b, 7 and 8). We believe that these could be of co-seismic origin.

- Other impressive fissures were also found 1 km SE from the previous site close to Fili fault (NE edge of Fili town, Aghios Kyprianos Monastery (Figure 1, site 3c). There the fault shows a huge high angle slope and typical weathered older fault surfaces (N130°–160°). The measured fissure started from the fault surface with a strike 160°–180° and was extended about 100 m inside the monastery. Heavy damages at the church (demolished) and other smaller settlements are due to this fracture, too. Some smaller breaks of few meters long trending almost parallel to main fault were in the soft materials. At the same site huge rocks have fallen from the highest parts on the sharp slope. All these are gravitational phenomena. Similar gravitational "breaks" observed near to the previous locality (1.5 km to the northwest) in both NE- and NW-directions, cutting across or parallel the country road are very superficial breaks of minor value.
- Open fissures (1–2 cm) were also observed within fault scarps on the limestone northern of Ano Liossia for few meters only (see map of Figure 1; site 3c and Figure 9a).
- A gravitational fissure about 300 m long at the base of an old, degraded scarp, heading N110°–N150° between Ano Liossia and Fili towns was the guideline which led to Fili fault (Figure 1, site 3e and 3d, Figure 5b). The fissure was about 2–4 cm wide (locally) and showed a minor normal displacement, down to the NE (Figure 1, 3e). The geographic coordinates of the antithetic rupture are at N38°05′47′′′, E023°40′56′′′. Note that the coordinates of the features have been marked using a hand-held Magellan 3000 GPS, which implies (Autumn 1999) a mean positional accuracy of 100 m.
- A characteristic of the sites 3a (Fili castle), 3b and 3d, where the possible coseismic fractures exist, are the stones and boulders thrown from their sockets during the main shock (Figure 10). They did not roll or slide on the surface, because they were lying on a flat level. Thrown stones and boulders in association with the high density of crack distribution and rock falls indicate high acceleration on the fault zone (see also Umeda, 1992).

All these seismic breaks are elongated WNW-ESE in the vicinity of the Fili fault. Some additional typical gravitational cracks were observed some kilometres northern on the NE- SW Athens basin marginal fault or mountain slopes (lift, road to the top of Parnitha mountain) (see Figure 1 for location site 1a and the photograph of Figure 9b).

5.3. NEOTECTONIC FAULT KINEMATICS AND STRESS FIELD

Since the kinematic history of a fault or a faulted area is defined mainly by kinematic indicators like striations contained on the fault surfaces, striation data were also collected from fault planes and the slickensides, striking N120° on average. They correspond to neotectonic and possibly active faults of the Fili broad area, e.g. from the fault surfaces shown in Figures 5–9, bearing polished fault planes cut-

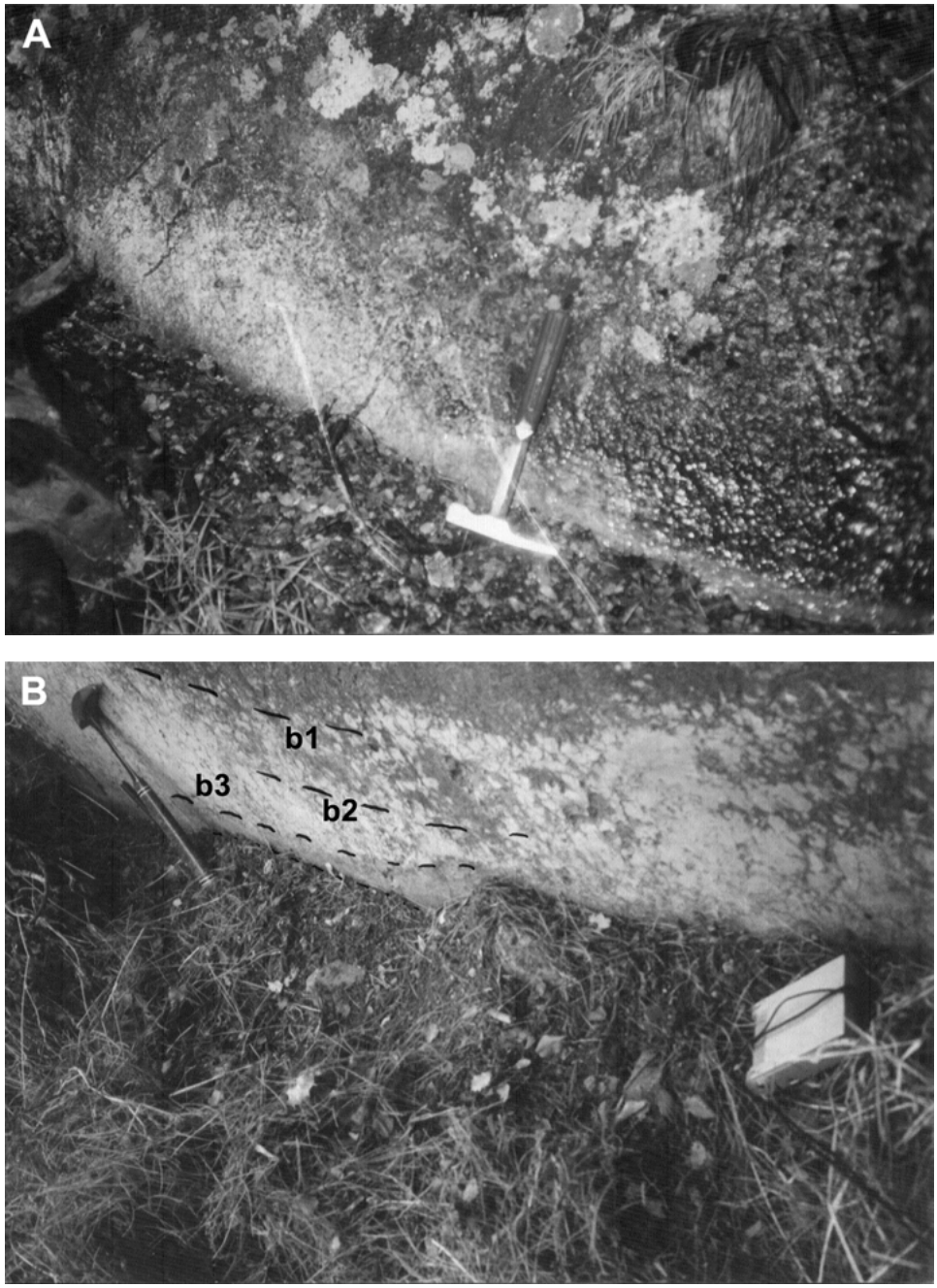

Figure 6. Light bands on the Fili polished fault surfaces (Triassic-Jurassic limestone). (a) close to Fili Fort (see Figure 1, site 3a for location), which was not created by the 1999 earthquake, but are indicators of possibly "older", still very young co-seismic displacements. (b) two similar light narrow zones, that is, "older" bands (b1 and b2, ~10 cm) and a third orange one (b3, ~6-8 cm) observed immediately after the earthquake (Fili fault, site 3b in Figure 1).

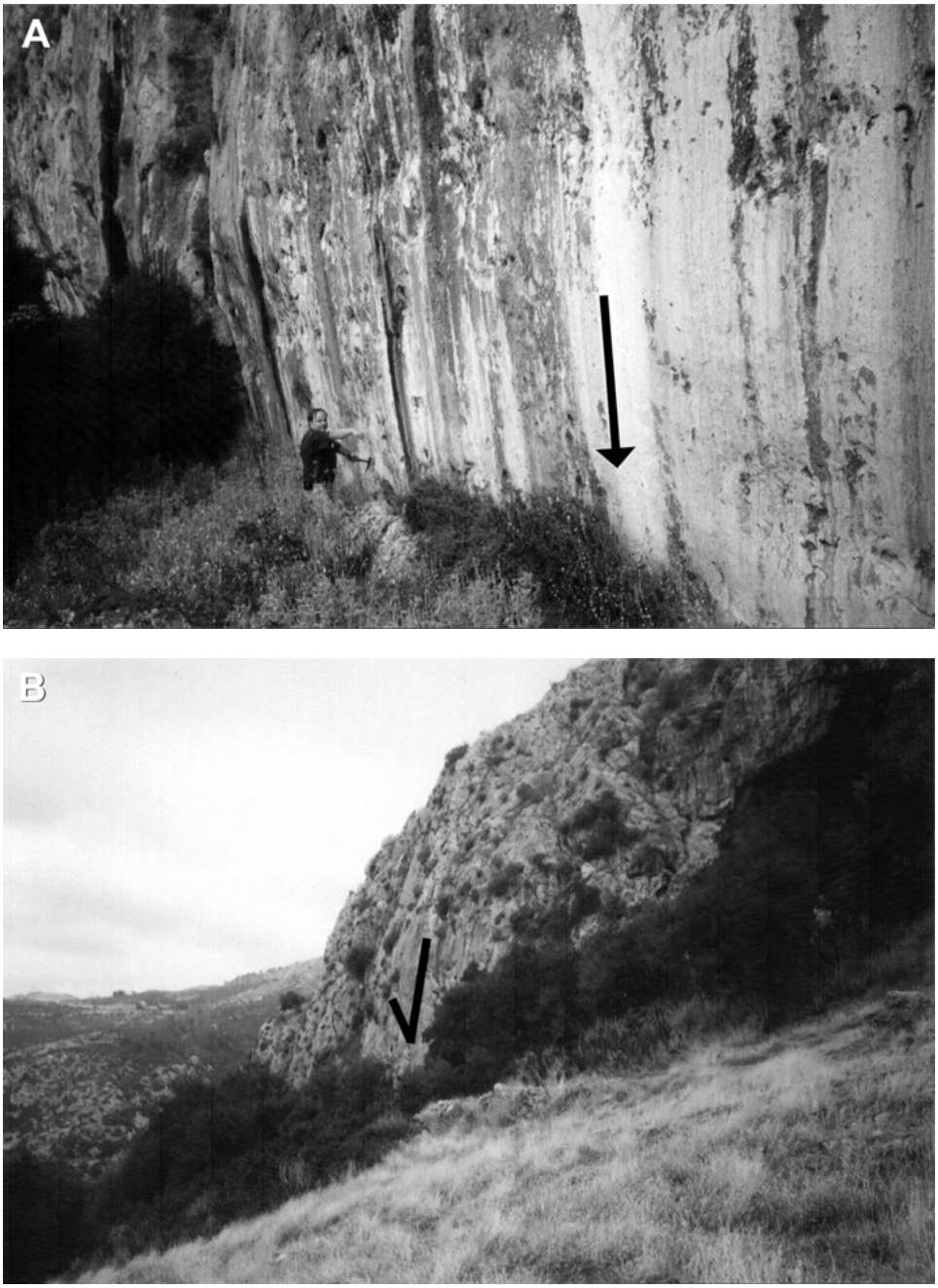

Figure 7. Field photographs of polished fault surfaces, WNW-ESE trending and SW dipping nearly vertical (Fili fault, Triassic-Jurassic crystalline carbonate rocks). For location, see Figure 1, site 3b. Arrows indicate the sense of movement (normal fault).

Figure 8. Field photographs. (a) polished fault surface and light band (site 3b in Figure 1, Fili fault) and (b) a possible co-seismic or triggered by the shock displacement along the same fault plane.

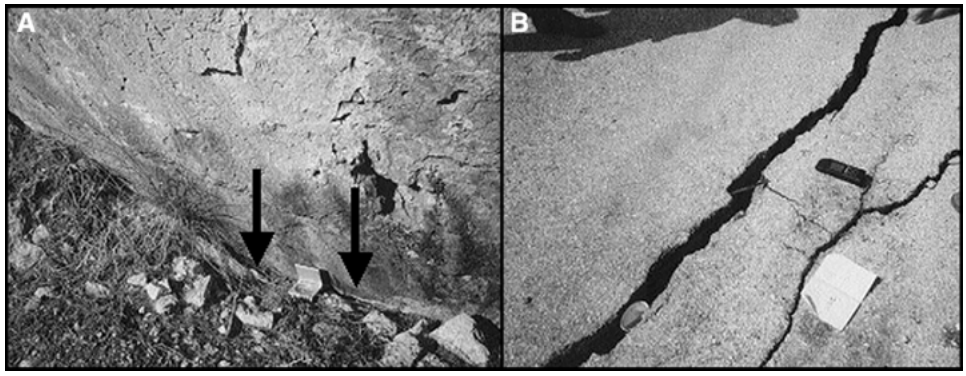

Figure 9. Field photographs which show ground dislocations. (a) open cracks (arrow) within the bedrock limestone (polished surface at Ano Liossia) along the SSE extension of Fili fault (site 3d in Figure 1). (b) gravitational fissures in the unconsolidated soft sediments covered by asphalt (Lift to Parnitha), along the NE-SW marginal structure of Athens basin (northwestern suburbs) (Figure 1, site 1a).

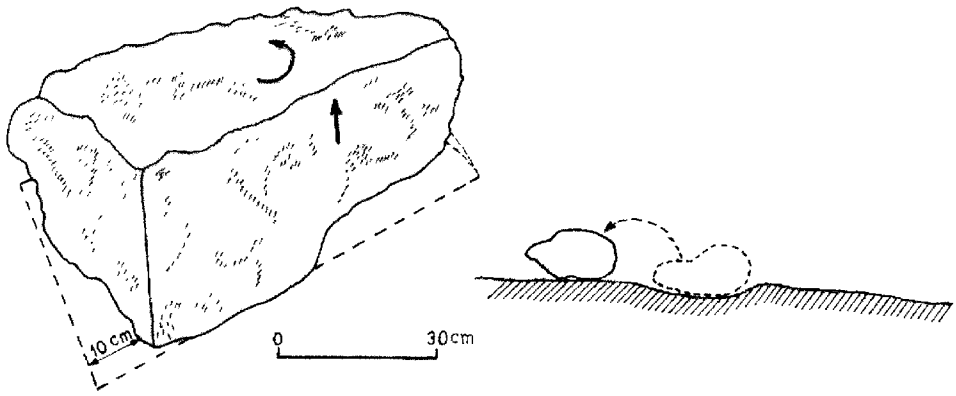

Figure 10. Examples of dislodged boulder (Fili Fort; see Figure 1, site 3a for location) and stone (Figure 1, site 3b, Fili fault). Stones have been thrown to a height equal to their diameter (∼15 cm) at least, while huge and heavy boulders thrown up a little and rotated counter clockwise (10 cm).

ting mainly trough basement crystalline carbonate rocks and occasionally through cemented limestone breccias. There are six fault groups, two from site 3a and four from sites 3b, 3c, 3d, 3e (Figure 1). The polished surfaces observed on the master neotectonic fault, indicate very young normal dip-slip movement reactivation with strikes ranging N110°–130°, SW dipping 54–85° and pitches of striation or rake −76° to −88° (Figures 11 and 12). The key to reconstruction of the principal palaeostress (ellipsoid) axes is to assume that movement on each fault is independent and occurs in the shear direction governed by a single common mean deviator. Fault planes and their striation were grouped in families and they were used to calculate the principal stress direction responsible for faulting, based on the Carey

and Brunier (1974) and Angelier (1979) methods with the "Conditioned Square Minima" technique of Caputo and Caputo (1998). The methods identify the driving stress ellipsoid, by determining the best fitting reduced palaeostress tensor for a given fault-slip data group. Examples of striated fault data and stress analysis are given in Figure 11 and the results are as follows (Strikes and Dips of the main stress axes):

Fili fault, (sites 3a in Figure 1)

σ_1 : N133°/76°, σ_2 : N312°/14°, σ_3 : N42°/0° (right dihedrons methodology)

σ_1 : N51°/69°, σ_2 : N306°/6°, σ_3 : N214°/20°(P/T axes methodology)

Fili fault (site 3b in Figure 1)

σ_1 : N76°/59°, σ_2 : N308°/21°, σ_3 : N209°/22°(right dihedrons methodology)

σ_1 : N58°/59°, σ_2 : N312°/9°, σ_3 : N217°/30°(P/T axes methodology)

Fili and NE-SW striking fault (site 3d in Figure 1)

σ_1 : N333°/69°, σ_2 : N84°/8°, σ_3 : N177°/19°(right dihedrons methodology)

σ_1 : N17°/78°, σ_2 : N109°/0°, σ_3 : N199°/12°(P/T axes methodology)

Tensional stress field with the σ_3 axis trending NNE prevails in the area and it is compatible with the focal mechanisms of the main shock (Figures 3 and 12), as well as with the broader regional stress field derived by quantitative neotectonic fault analysis and focal mechanisms (e.g., Mercier *et al.*, 1989; Caputo and Pavlides,1993; Papazachos and Kiratzi,1996; Roberts and Ganas, 2000). Concerning the fault dip a value of 56° has been accepted (Figure 13), although at surface level, we have measured bigger dip values. It is common for normal faults to have surface expression of about 80°, especially on carbonate formations, as in this case, and especially in the broader Aegean region (see Stewart and Hancock, 1988, 1991). Their lower dip at depth has been explained as listric or angular geometry.

6. Concluding Remarks

This earthquake is relatively small compared to the other strong events that occurred in mainland Greece in the last twenty years or so, but it is of great social significance for the Athens Metropolitan area. It could be considered as the most destructive event in Greece in modern times. Due to its moderate size and absence of typical seismic ruptures at the surface, the identification of the topographic expression of the seismogenic structure is a complex and difficult problem. This requires a multi-disciplinary approach as the normal fault which caused the event

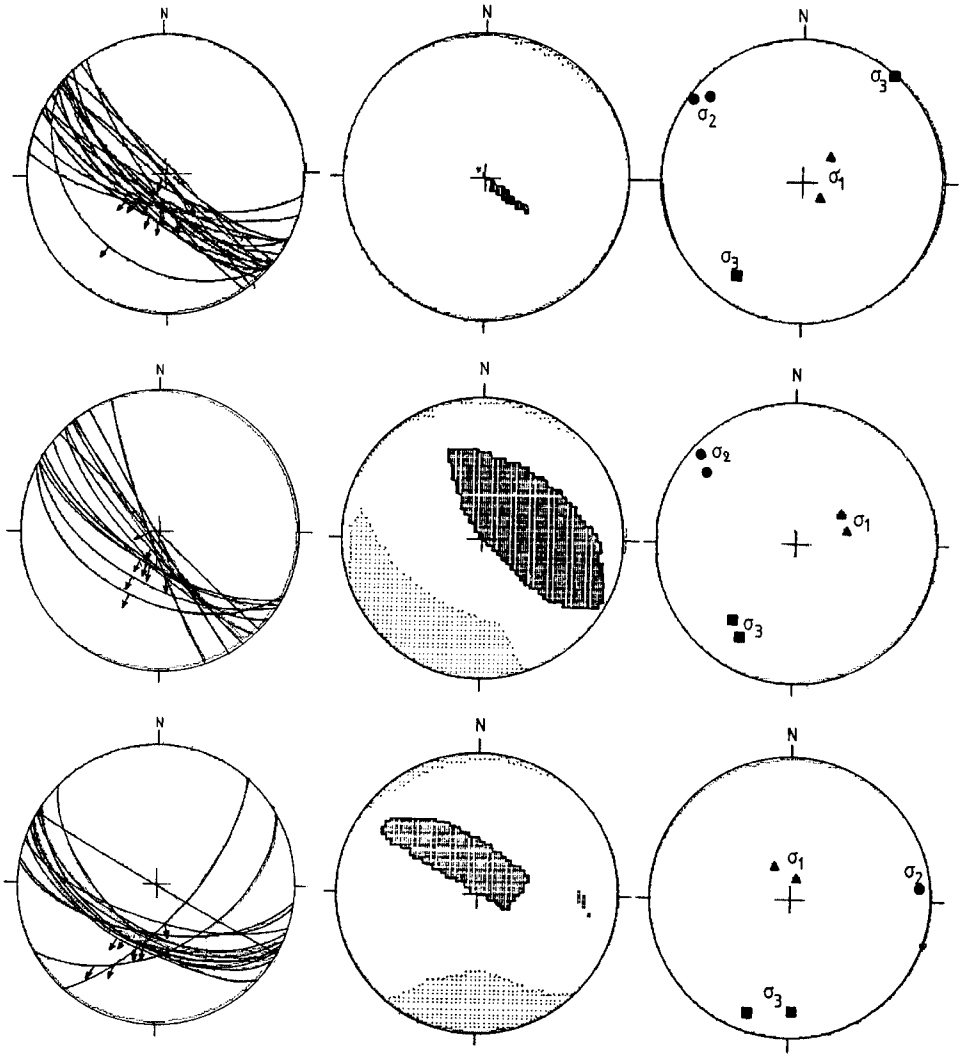

Figure 11. Fault kinematics: quantitative paleostress (neotectonic) analysis along the Fili fault (sites 3a, 3b, 3d in Figure 1). Column A: Striated faults are presented in stereographic projection (lower hemisphere) as major cycles (curves) and striation as small arrows (normal sense of movement). Column B: Application of the right-dihedrons method where black is the area of 100% containing σ_1 (or P) axis and light colour areas (dots) of 100% containing σ_3 (or T) axis. Column C: The application of Caputo and Caputo (1989) P-T axes methodology for determination of σ_1 (compressional-triangles), σ_2 (intermediate-circles) and σ_3 (tensional-squares).

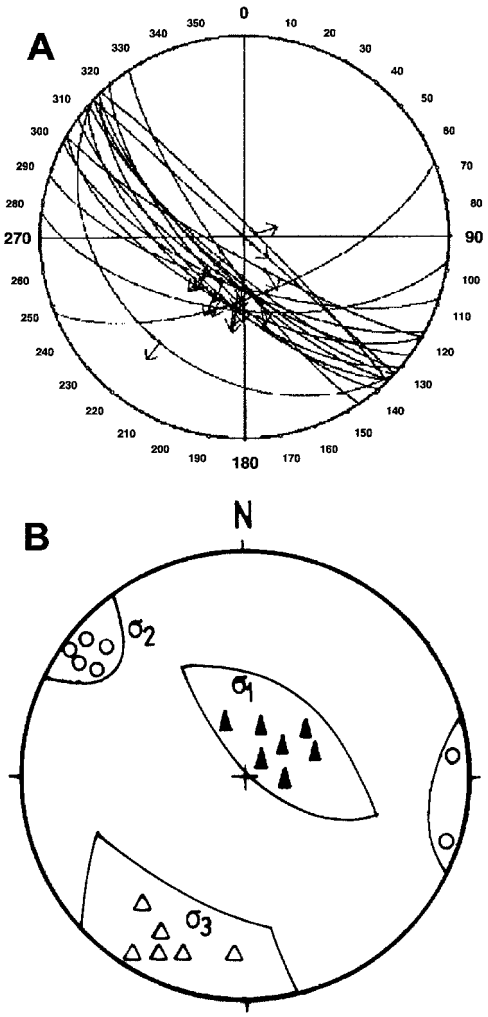

Figure 12. (a) Striate fault surfaces in an equal-area, lower hemisphere stereographic projection, measured along the Fili fault. They are a group of representative of the best striated (quality A) faults surfaces. Fault-planes are shown as great circles and striation as arrows. They range from ENE-WSW to SSE-NNW directions (best N115–130° and mean dip 70°SW). (b) Stereographic projection (lower hemisphere) of stress axes σ_1 as heavy triangles, σ_2 as open circles, and σ_3 as open triangles, calculated from six sites along the Fili fault (see Figure 11). This analysis has been based on the Carey and Brunier (1974), Angelier (1979) and Caputo and Caputo (1988) methodologies. Comparison of the paleostress axes σ_1, σ_2, σ_3 with the corresponding P, T, B axes are derived from the focal mechanism of the 7 September 1999 earthquake (Figure 3).

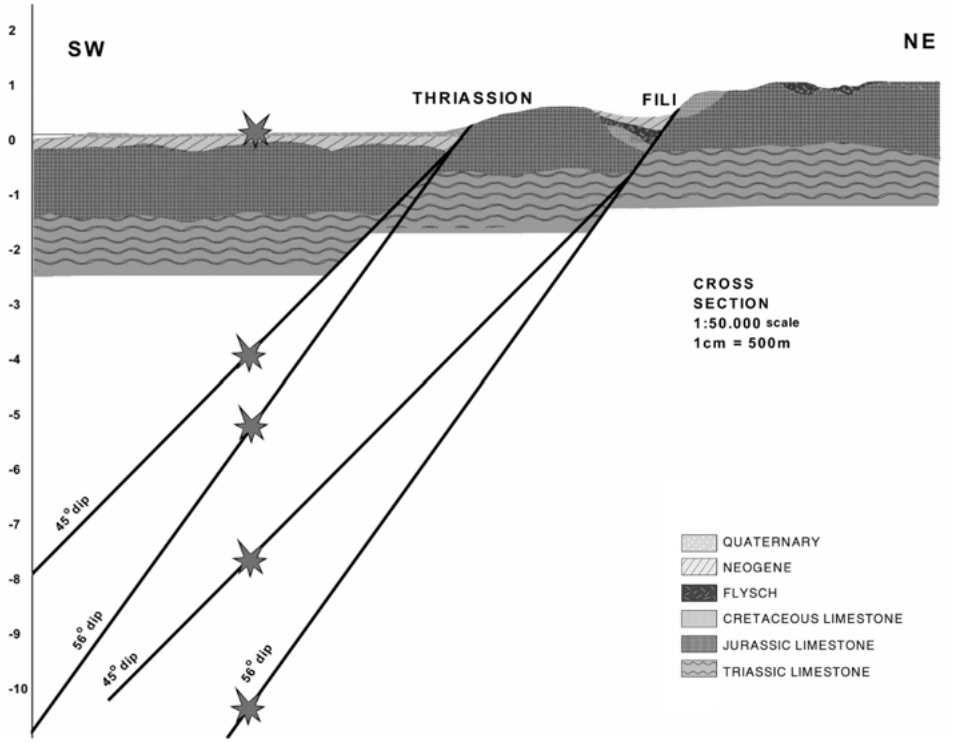

Figure 13. Geological cross section (NE-SW, AA′ in Figure 1). Fili and Thriassion faults are shown (dip ranges 45-56 degrees, respectively) in relation to the epicenter-hypocenter of the earthquake. Legend follows the IGME (1980) map.

was previously unidentified. Therefore, immediately after the occurrence of the earthquake, the following methodologies and techniques were applied: (a) Field observations, mapping and fault measurements along the three main faults of the epicentral area (Table I); (b) Morphotectonic approaches, using also 20-m Digital Elevation Models, (c) Landsat imagery interpretation; d) Macroseismic effects evaluation; and (e) Aftershock distribution data and focal mechanisms solutions of the main shock were also taken into consideration. Additional data came from radon soil emission measurement some days after the earthquake (IGME, G. Vougoukalakis, personal communication), which are concentrated mainly along the eastern edge of the Fili fault. A comparative picture of the criteria used is given in Table I.

Geodesy and SAR interferometry could be the last methods to be applied in order to map the ground deformation in more details. The results of Kontoes *et al.* (2000) suggest that the activation of a fracture zone located at the Fili broad area (southern Parnitha mountain), is more likely associated with the Athens earthquake, resulting in the observed surface deformations (*ERS-2 Satellite Radar Interferometry*). According to their model the main fault segment is located at the

Table I. Summary of geomorphic and seismotectonic criteria applicable to the selection of the seismogenic structure

Criteria	NE fault	Thriassion fault	Fili fault
Focal mechanism – N120°		V	V
Aftershock distribution NW-SE		V	V
Epicentre location – Thriassion		V	V
Epicentre distance to fault			V
12 km for 45°			
8.4 km for 55°			
Damage distribution	V		V
VIII–IX(MMI)			
Quaternary basin	V	V	V
Previous earthquakes (?)			
Rocks falls - limestone	V		V
Surface breaks cm size gravitational	V		V
Destruction Fili Fort			V
(400 BC) Hanging wall			
Remote sensing > 10 km		V	V
Radon emission (IGME)			V
Interferometry (Kontoes *et al.*)			V

NW extension of the Fili fault, as mapped by Pavlides *et al.* (1999), while the eastern branch does not fit well with surface neotectonic structures. So, Kontoes *et al.* (2000) introduce a secondary smaller parallel seismogenic fault. Additionally, aftershock data show an activation of high angle fault (or faults) at depths of 3 to 16 km (Papadopoulos *et al.*, 2000), which did not create typical surface co-seismic traces. The absence of shallow seismic activity prevented the rupture propagation towards the earth surface and hindered the direct identification of the seismogenic fault. The gravitational phenomena and especially the small but clear displacements observed for some tens of metres along the Fili fault could be considered as triggering superficial phenomena on the seismogenic structure. The hypothesis of "blind fault" must be excluded, because the Fili fault, which fits better with aftershock distribution, focal mechanism, and ground deformation, is the most and only typical active fault in the area.

Thus, the co-seismic structure of the Athens September 1999 shock, which fulfill all the criteria, that is field and instrumental data (Table I), can be identified as the 8 km long, WNW-ESE striking and SW dipping Fili fault, which possibly extends 2 to 5 km ESE towards the Athens' suburbs Ano-Liossia and Acharnai (Figs. 1 and 2), where its geometry is not well known. Aftershock distribution

indicates a longer 20–30 km seismogenic structure at depth (Papadopoulos *et al.*, 2000).

The Athens 1999 earthquake is a "floating" or "random event" according to the terminology of de Polo and Slemmons (1990). That is an earthquake that is usually a small-to-moderate event (magnitude range 5 to 6.5) that can occur anywhere in a region or area. Moderate size floating earthquakes occurring close to urban areas are of major concern, as it occurred in the Athens Metropolitan area. Moreover, the Athens event poses once more fundamental questions that are yet to be answered. Was this fault detectable before the earthquakes? What is the likelihood of occurrence of small/medium earthquakes near densely populated areas? What is the earthquake potential of fault segments previously regarded as inactive, are still active? What type of data is needed to assess the vulnerability of big cities? The M 5.9 event caused very strong ground motion and consequently extreme damage in Athens, due to the location of the epicentre and the direction of propagation of the rupture from west to east, that is, rupture propagation westwards of extensive residential zones of the city. However, it is reasonable that the heavy damage can be partly explained by inferring a southeastern extension of the fault beneath the western suburbs of the city. It remains to be seen if the Fili fault tip fades out somewhere in the Athens basin, or similar structures occur further to the southeast or some small antithetic and sympathetic fault activated.

A new factor that should be carefully examined in active fault studies is that posed by the needs of modern society, which is urbanisation. Even relatively small or moderate earthquakes can be very destructive when striking densely populated regions, as it happened at Athens, when small-scale active structures appear proximal to urbanised areas. These areas should be considered of high risk and should be treated accordingly.

Acknowledgments

This paper has been written within the frame of the research project ASPELEA (Assessment of Seismic Potential in European Large Earthquakes Areas), supported by the Commission of European Communities – DG XII, INCO – COPERNICUS Program, contribution IC – 15CT – 97 – 0200 and partly by the General Secretary of Research and Technology, Greece. Raw Landsat TM data were supplied from the archive of IIS SA. All image processing was done using EASI PACE v6.3 for Windows NT. Thanks are also due to I. Koukouvelas and to three anonymous reviewers who have helped to improve the manuscript.

References

Ambraseys, N. N.: 1994, Material for the investigation of seismicity of central Greece. Materials CEC project, In: Albini and Moroni (eds.), *Review of Historical Seismicity in Europe*, Vol. 2, pp. 1–10.

Ambraseys, N. N. and Jackson, J. A.: 1990, Seismicity and associated strain of central Greece between 1890 and 1988, *Geophysical Journal International* **101**, 663–708.

Ambraseys, N. N. and Jackson, J. A.: 1998, Faulting associated with historical and recent earthquakes in the Eastern Mediterranean region, *Geophys. J. Int.* **133**, 390–406.

Angelier, J.: 1979, Determination of mean principal detection of stresses for a given fault population, *Tectonophysics* **56**, T17–T26.

Caputo, M. and Caputo, R.: 1988, Structural analysis: New analytical approach and applications, *Ann. Tectonicae* **2**(2), 84–89.

Caputo, R.: 1993, Morphotectonics and kinematics along the Tyrnavos Fault, northern Larissa Plain, mainland Greece, In: I. Stewart, C. Vita-Finzi, and L. A. Owen (eds.), *Neotectonics and Active Faulting*, Zeitschrift fur Geomorphologie N.F., Suppl.-Bd. 94, Stuttgart, pp. 165–183.

Caputo, R. and Pavlides, S.: 1993, Late Cenozoic geodynamic evolution of Thessaly and surroundings (central-northern Greece), *Tectonophysics* **223**, 339–362.

Carey, F. and Brunier, B.: 1974, Analyse theorique et numerique d'un modele mecanique elementaire appliquĆ a l'edute d'une population de failles, *C. R. Acad. Sci. Paris* **279**, 891–894.

Coppersmith, K. and Young, R. R.: 2000, Data needs for probabilistic fault displacement hazard analysis, *J. Geodynamics* **29**, 329–343.

DePolo, M. C. and Slemmons, B. D. (1990). Estimation of earthquake size for seismic hazards. *Geol. Soc. Amer. Rev. Engin. Geol.* **VIII**, 1–28.

Freyberg, B. V.: 1951, Das Neogen-Gebiet nordwestlich Athen, *Ann. Geol. Pays Hellen.* **III**, 65–86.

Ganas, A. and Athanassiou, E.: 2000, A comparative study on the production of satellite orthoimagery for geological remote sensing, *Geocarto International* **15**(2), 51–59.

Galli, P. and Galadini, F.: 1999, Seismotectonic Framework of the 1997–1998 Umbria-Marche (Central Italy) earthquakes, *Seismological Research Letters* **70**(4).

IGME: 1980, Geological map of Greece, "Athinai-Elefsis" sheet (1:50,000).

Jackson, J.: 1999, Fault death: A perspective from actively deforming regions, *J. Struct. Geol.* **21**, 1003–1010.

Jackson, A. J., Gagnepain, J., Houseman, G., King, G. C. P., Papadimitriou, P., Soufleris, C., and Virieux, J.: 1982, Seismicity, normal faulting, and the geomorphological development of the Gulf of Corinth (Greece): The Corinth earthquakes of February and March 1981, *Earth and Planetary Science Letters* **57**, 377–397.

Kontoes C., Elias, P., Sykioti, O., Briole, P., Remy, D., Sachpazi, M., Veis, G., and Kotsis, I.: 2000, Displacement field and fault modeling for the September 7, 1999 Athens earthquake inferred from Ers-2 satellite radar interferometry, *Geophysical Research Letters* **27**(24), 3989–3992.

Leeder, M. R. and Jackson, J. A.: 1993, The interaction between normal faulting and drainage in active extensional basins, with examples from western United States and central Greece, *Basin Research*, **5**, 79–102.

Louvari, E. and Kiratzi, A.: 2001, Source parameters of the September 7, 1999 Athens (Greece) earthquake based on teleseismic data, *Journal of Balkan Geophysical Society* **4**, 51–60.

Meghraoui, M., Bosi, V., and Camelbeeck, T.: 1999, Fault fragment control in the 1997 Umbria-Marche, central Italy, earthquake sequence, *Geoph. Research Letter* **26**(8).

Mercier, J.-L., Sorel, D., Vergely, P., and Simeakis, K.: 1989, Extensional tectonics regimes in the Aegean Basins during the Cenozoic, *Basin. Res.* **2** 49–71.

Michetti, A.M., Ferreli, L., Esposito, E., Porfido, S., Blumetti, A. M. Vittori, E., Serva, L., and Roberts, G. P.: 2000, Ground effects during the September 9, 1998, Mw = 5.6, Lauria earthquake and the seismic potential of the aseismic Pollino region in Southern Italy, *Seismological Research Letters* **71**(1), 31–46.

Papadimitriou, P., Kaviris, G., Voulgaris, N., Kassaras, I., Delibasis, N., and Makropoulos, K.: 2000, The September 7, 1999 Athens earthquake sequence recorded by the cornet network: Preliminary results of source parameters determination of the mainshock, *Ann. Geol. Pays Hellen. Memoire J. Drakopoulos, 1e serie* **T. XXXVIII**(Fasc, B.), 29–39.

Papadopoulos, G. A., Drakatos, G., Papanastassiou, D., Kalogeras, I., and Stavrakakis, G.: 2000, Preliminary results about the catastrophic earthquake of 7 September 1999 in Athens, Greece, *Seism. Res. Letters* 71, 318–329.

Papazachos, B. C. and Kiratzi, A. A.: 1996, A detailed study of the active crustal deformation in the Aegean and surrounding area, *Tectonophysics* **253**, 129–153.

Pavlides, S. B. and King, G. C. P.: 1998, The 1995 Kozani–Grevena earthquake (N. Greece): An introduction, In: S. Pavlides and G. King (eds.), *J. Geodyn. Spec. Issue*, Vol. 26, Nos. 2–4, pp. 171–173.

Pavlides, S., Papadopoulos, G. A., and Ganas, A.: 1999, The 7th September, 1999 unexpected earthquake of Athens: Preliminary results on the seismotectonic environment, *1st Conf. Advances in Natural Hazards Mitigation: Experiences from Europe and Japan, Programme-Abstracts-Reports*, 3–4 November, 1999, Athens, pp. 80–85.

Pavlides, S., Caputo, R., and Chatzipetros, A.: 2000a, Empirical relationships among earthquake magnitude, surface ruptures and maximum displacement in the broader Aegean region, In: Panayides *et al.* (eds.), *Proc. 3rd igcem (Intern. Geolog. Congress on the Eastern Mediteranean)*, September 1998, Nikosia, Cyprus, pp. 159–168.

Roberts, G. P. and Ganas, A.: 2000, Fault-slip directions in central and southern Greece measured from striated and corrugated fault planes: Comparison with focal mechanism and geodetic data, *J. Geophys. Res.* **105**(B10), 23443–23462.

Sargeant, S.L., Burton, P.W., Douglas, A., and Evans, J.R. : 2000, *A Source Model for the 7th September 1999 Athens Earthquake*, XXVII General assembly of the European Seismological Commission (ESC), Lisbon, Portugal, Abstracts and papers, pp. 138–159.

Stewart, I. S.: 1993, Sensitivity of Fault-generated scarps as indicators of active tectonism: Some constraints from the Aegean region. In: D. S. G. Thomas and R. J. Allison (eds.), *Landscape Sensitivity*, John Wiley and Sons Ltd.

Stewart, I. S. and Hancock, L. P.: 1988, Normal fault zone evolution and fault scarp degradation in the Aegean region, *Basin Research* **1**, 139–153.

Stewart, I. S. and Hancock, P. L.: 1991. Scales of structural heterogeneity within neotectonic normal fault zones in the Aegean region, In: Hancock *et al.* (eds.), *Characteristics of Active Faults*, J. Struct. Geol., Vol. 13, pp. 191–204.

Stiros, S. C.: 1995, The 1953 seismic surface fault implications for the modeling of the Sousaki (Corinth area, Greece) geothermal field, *Journal of Geodynamics* **20**, 167–180.

Tselentis, G. A. and Zahradnik, J.: 2000, Aftershock monitoring of the Athens earthquake of 7 September 1999, *Seism. Res. Lett.* **71**, 330–337.

Umeda, Y.: 1992, The bright spot of an earthquake, *Tectonophysics* **211**, 13–22.

Vittori, E., Deiana, G., Esposito, E., Ferreli, L., Marchegiani, L., Mastrolorenzo, G., Michetti, A. M., Porfido, S., Serva, L., Simonelli, A. L., and Tondi, E.: 2000, Ground effects and surface faulting in the September–October 1997, Umbria – Marche (Central Italy) seismic sequence, *Journal of Geodynamics* **29**(3–5), 535–564.

Voulgaris, N., Kassaras, I., Papadimitrou, P., and Delibasis, N.: 2000, Preliminary results of the Athens September 7, 1999, aftershock sequence, *Ann. Geol. Pays Hellen. Memoire J. Drakopoulos, 1e serie* **T. XXXVIII**(Fasc, B.), 51–62.

Wells, D. L. and Coppersmith, J. K.: 1994, New empirical relationships among magnitude, rupture length, rupture width, rupture area, and surface displacement, *Bull. Seism. Soc. Am.* **84**(4), 974–1002.